

Magnetic field sensors using large cat states beyond the standard quantum limit

Stephanie Simmons,^{1,*} Jonathan A. Jones,² Steven D. Karlen,¹ Arzhang Ardavan,² and John J. L. Morton^{1,2}

¹*Department of Materials, Oxford University, Oxford OX1 3PH, United Kingdom*

²*CAESR, Clarendon Laboratory, Oxford University, Oxford OX1 3PU, United Kingdom*

Measurement devices could benefit from entangled correlations to yield a measurement sensitivity approaching the physical Heisenberg limit. Building upon previous magnetometric work using pseudo-entangled spin states in solution-state NMR, we present two conceptual advancements to better prepare and interpret the pseudo-entanglement resource as well as the use of a 13-spin cat state to measure the local magnetic field with a sensitivity beyond the standard quantum limit.

Many technologies are looking to quantum mechanics as a way to dramatically improve upon current capabilities [1, 2]. As examples, interferometry [3, 4, 5], metrology [6], lithography [7], and information processing [8, 9, 10] are pursuing quantum information techniques to make use of the benefits of highly correlated entangled states. Even environments which normally use the pseudopure approach such as Nuclear Magnetic Resonance (NMR) [11, 12, 13, 14] can exploit a pseudo-entanglement resource for highly sensitive magnetic field measurements [15].

In a locally homogeneous magnetic field, an isolated nuclear spin will precess according to its Larmor frequency which depends only on the nuclear species and the magnetic field [16]. Consider the (unnormalised) state $|0\rangle + |1\rangle$ in a rotating frame, where the states $|0\rangle$ and $|1\rangle$ refer to the parallel and anti-parallel spin eigenstates. After a time t such a state would evolve into the state $|0\rangle + \exp(i\gamma B_0 t) |1\rangle$, where the gyromagnetic ratio γ is known, so the acquired phase can be used to deduce the local magnetic field B_0 . A set of N isolated spins can therefore serve as microscopic magnetic field sensors [16], with a measurement sensitivity proportional to \sqrt{N} . This degree of precision is known as the ‘standard quantum limit’ [17].

It is possible to exceed this limit by making use of quantum entanglement. If we assemble the N spins in the state $|\mathbf{0}\rangle + |\mathbf{1}\rangle = |00\dots 0\rangle + |11\dots 1\rangle$, this will evolve, after a time t , into the state $|\mathbf{0}\rangle + \exp(iN\gamma B_0 t) |\mathbf{1}\rangle$. This evolution allows us to determine B_0 with an increased sensitivity compared to measuring each spin’s evolution independently. The degree of sensitivity approaches the fundamental Heisenberg uncertainty relation [18], in that we are theoretically able to have a sensitivity proportional to N using N particles.

We recently reported proof of principle experiments exploiting pseudo-entanglement in nuclear spin ensembles [15]. In this Letter we grow the size of the cat state from 10 to 13 spins and address some limitations of the previous approach. Specifically, we incorporate a polarisation-priming sequence that more intelligently exploits the pseudo-entanglement resource and additionally disconnect the centre spin during field measurement to simplify the field estimation.

To quickly generate large states such as $|\mathbf{0}\rangle + |\mathbf{1}\rangle$, referred to as ‘NOON’ [4] or ‘cat’ [19, 20, 21, 22] states, we chose natural abundance solution-state tetramethylsilane (TMS) as our sensor compound. We sought a central spin-active nucleus distinct from, and surrounded by, many chemically equivalent outer spin-active nuclei, allowing us to address all peripheral spins globally; this highly symmetric configuration means that the pulse sequence complexity is independent of the number of spins, in contrast with previous work [19, 20, 21]. Roughly 4.7% of the molecules consist of one ^{29}Si spin surrounded by twelve ^1H spins (isotopic labeling could in principle be used to increase this proportion, but was not used here). Such a molecule is capable of hosting a 13-spin ‘cat’ state.

Reading out the thermal state on the centre ^{29}Si spin produces thirteen peaks corresponding to the distribution of up and down spins in the nearby hydrogen nuclei. It is convenient to assign a number, ℓ , to each of these peaks corresponding to their ‘lopsidedness’, that is $\ell = u - d$ where u and d are the number of intramolecular up and down proton spins, respectively.

The basic sequence consists of a Hadamard gate on the centre spin to generate the state $|\mathbf{0}\rangle + |\mathbf{1}\rangle$, a controlled-not (CNOT) gate conditional upon the state of the centre spin, followed by an evolution delay t before reversing the previous CNOT so that the final phase is mapped onto the centre spin for readout. This sequence can either be applied to a pseudopure state (corresponding to a single peak) or the entire thermal state (all thirteen peaks with a Boltzmann distribution of intensities). The two methods are computationally equivalent, but starting from the thermal state gives a stronger readout signal. The internal peaks will usefully pick up phase proportional to their lopsidedness [15]. The application of the sensor sequence to the internal lines generates states that are not quite ‘NOON’ states — the term ‘Many-Some, Some-Many’ (or ‘MSSM’) was introduced [15] to describe these states.

In this scheme the phase acquired by each peak, identified by its lopsidedness ℓ , is given by

$$\phi/t = B_0 (\ell\gamma_{\text{H}} + \gamma_{\text{Si}}) \quad (1)$$

where $\gamma_{\text{H}} = 42.577 \text{ MHz/T}$ and $\gamma_{\text{Si}} = -8.465 \text{ MHz/T}$ are the gyromagnetic ratios of ^1H and ^{29}Si , respectively. As NMR experiments are most conveniently described

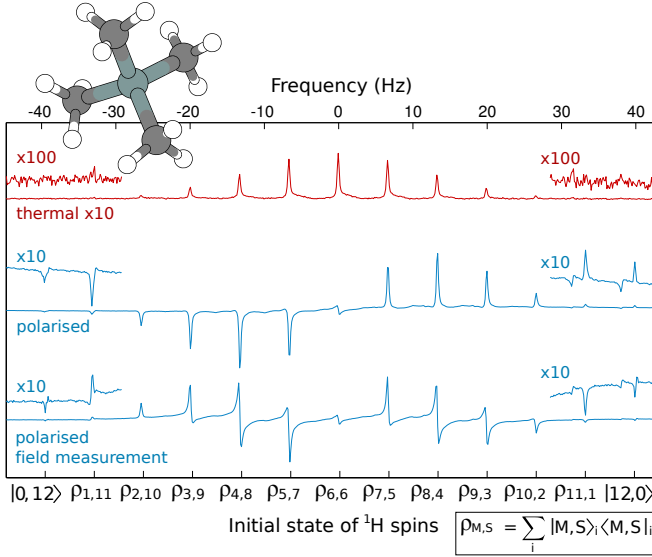


FIG. 1: **Priming the 13-spin MSSM states (created using the 12 hydrogen spins (white) and the centre ^{29}Si spin (blue) in TMS) is critical for large sensors. The three ^{29}Si spectra show how the polarisation of each thermally equilibrated MSSM state (red) can be amplified according to its lopsidedness with polarisation priming (blue). Each primed MSSM state can then be used for field measurement, where the very lopsided outermost peaks evolve more rapidly (and are hence more sensitive) than the inner peaks.**

in a rotating frame [16] the observed phase depends not directly on the magnetic field but rather on its offset B_0 from some assumed nominal value. With this in mind we can calculate the phase sensitivity increase of TMS to be 61.4 over an individual silicon spin and 12.2 over a single hydrogen spin.

The Boltzmann distribution of populations of the ^1H spins leads to weak intensities for the outermost MSSM lines which are the most sensitive to magnetic field. This could be addressed by physically [23] or computationally [24] manipulating the sensor molecule. We now describe a simple approach which uses the quantum resource more efficiently than simply averaging many measurements.

Many techniques for polarisation transfer have been developed in NMR systems [25]; these work not by increasing the polarisation, but instead by transferring polarisation from one part of the density matrix to another where it can be more effectively used. One simple example is a CNOT gate applied to a high γ nucleus controlled by a low γ nucleus, which transfers the population difference across a transition of the high γ nucleus to a low γ transition, effectively multiplying the polarisation of the insensitive nuclei by γ_R , the ratio of the gyromagnetic ratios of the two nuclei. (In conventional NMR experiments this is known as InSENSITIVE NUCLEI ENHANCED BY POLARISATION TRANSFER (INEPT) [25, 26]). In our highly symmetric molecular sensor, the amplitude benefits of polarisation

transfer are even greater than this ratio ($\gamma_R = -5.03$) as the CNOT has the effect of increasing the signal in a negative direction for each coupled ‘up’ ^1H spin (negative because γ_R is negative) and positive direction for each connected ‘down’ ^1H spin. Explicitly, a peak of lopsidedness ℓ in a polarisation-primed sensor undergoes an amplitude magnification A according to

$$A(\ell) = (1 + \gamma_R \ell) \quad (2)$$

This means the outermost lines—the most sensitive components of the sensor with the poorest thermal populations—are those most amplified by the polarisation transfer. The integrated intensities of the outermost lines display an approximately 60-fold increase over the thermally-polarised measurement as expected.

Polarisation-priming provides another advantage: by swapping the polarisation of sensitive and insensitive nuclei, one only needs to wait for the sensitive nuclei to rethermalise. Although the details of relaxation processes can be complicated, in fast-tumbling spin-1/2 systems dominated by dipolar relaxation the T_1 time is inversely proportional to the square of the gyromagnetic ratio [16], so as the polarisation-priming sequence enhances the polarisation it also decreases the rethermalisation time. A field estimation generated from the basic sequence with polarisation priming is shown in Figure 1.

Instrumentally, there will always be some error associated with imperfect frequency detunings. Equation 1 assumes that the frequencies of the ^1H and ^{29}Si channels have been chosen correctly, so that they are precisely on resonance with their respective nuclei at the nominal field strength. In general:

$$\phi/t = B_0 (\ell \gamma_H + \gamma_{Si}) + (\ell \delta_H + \delta_{Si}) \quad (3)$$

where δ_H and δ_{Si} are the frequency offsets of the nuclei at the nominal field. One can mitigate the errors generated by these terms by systematically removing them. One of these offsets (here assumed to be δ_H) can be eliminated by shifting the nominal field, but it is only possible to remove both terms if the frequencies are set correctly. An imprecisely known rotating frame offset leads to inaccurate field estimations. This requirement can be removed by ‘disconnecting’ (disentangling) the centre spin during the phase acquisition delay. Two methods for achieving this are introduced in Figure 2.

Consider how sequence A acts upon the leftmost line. In the pseudopure approximation [13] the leftmost line in its thermal state is represented as $|0\rangle_{Si} |0\rangle_H^{\otimes 12}$, where \otimes indicates a tensor product. A Hadamard gate followed by a CNOT gate conditional upon the silicon nucleus transforms the initial state into $|0\rangle_{Si} |0\rangle_H^{\otimes 12} + |1\rangle_{Si} |1\rangle_H^{\otimes 12}$. It is here that we can disentangle the central ^{29}Si spin from our large cat state by applying a NOT gate to ^{29}Si in the second term, giving

$$|0\rangle_{Si} |0\rangle_H^{\otimes 12} + |0\rangle_{Si} |1\rangle_H^{\otimes 12} = |0\rangle_{Si} (|0\rangle_H^{\otimes 12} + |1\rangle_H^{\otimes 12}) \quad (4)$$

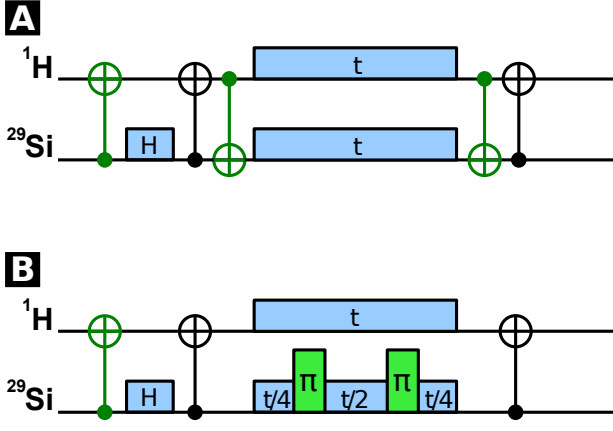


FIG. 2: The two field sensor sequences with all improvements (coloured green) presented in this paper. The polarisation-priming component begins the sequence with appropriate delays $\Delta = 1/4J$ for J the spin-spin coupling constant. In Sequence A, the centre two CNOT gates are ‘disentangling’ gates designed to allow only one nuclear species (${}^1\text{H}$ in TMS) to evolve during measurement. In Sequence B, two π pulses separated by half the delay t emulates a disentangling effect by reversing the phase acquired by that nucleus for half of the phase acquisition time.

so that only the ${}^1\text{H}$ spins will acquire field-dependent phases.

It might seem that this approach would require a multiply-controlled NOT gate (a generalised Toffoli gate), but with a pseudopure state this is not required. It is only necessary to apply a NOT gate to the second term and *not* to the first term. This can be achieved with a modified CNOT gate [14], with the evolution time chosen to match the separation between the outermost lines in the ${}^{29}\text{Si}$ multiplet rather than the conventional coupling size.

This simple approach must be modified to work simultaneously with a general set of MSSM lines. With an odd number of ${}^1\text{H}$ spins, this can be achieved with a conventional CNOT gate (see Figure 2A), which disentangles every MSSM line. This approach does not work for systems with an even number of ${}^1\text{H}$ spins. An alternative, simpler method (Figure 2B) uses echoes to refocus the inner ${}^{29}\text{Si}$ spin rather than disentangling it, and this can be applied to both even and odd systems. Under both sequences we read out the acquired phase by applying the sequence in reverse, and observing the central ${}^{29}\text{Si}$ spin.

To test this approach, we applied a small offset to the ${}^{29}\text{Si}$ channel and implemented a full field estimation with the original pulse sequence and with the modified sequence B. As shown in Fig. 3, the field estimation now gives slightly different results for different lines in the multiplet if the original sequence is used, but these im-

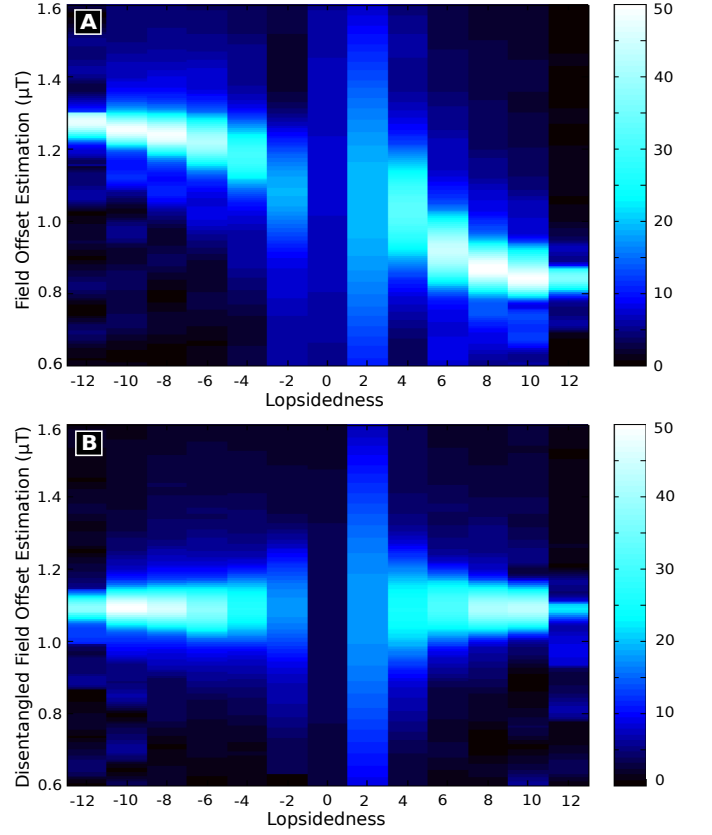


FIG. 3: Each peak in the ${}^{29}\text{Si}$ NMR spectrum (labeled according to lopsidedness) can estimate the local magnetic field. The precision of each peak’s estimation scales according to its absolute lopsidedness, leading to the most precise estimations at the outermost peaks. The colour amplitude chosen reflects the gain in signal from the polarisation-priming sequence; a value of 1 on each peak estimation represents its thermal binomial amplitude (See Equation 2). **A:** The field estimation is visibly sensitive to a small nonzero detuning (3.5 Hz) on the ${}^{29}\text{Si}$ spin if it is not disentangled during measurement. **B:** The same ${}^{29}\text{Si}$ detuning does not distort the field estimation when applying disentangling sequence B (see Figure 2B)

perfections are removed by the modified sequence. We then repeated the phase estimation with a wide range of silicon channel detunings (data not shown) and obtained indistinguishable field estimations. Sequences A and B were both successfully implemented on our original odd spin system, trimethylphosphite (data not shown).

The most obvious drawback of these new sequences is a mild sensitivity decrease from $(12\gamma_H + \gamma_{Si})/\gamma_H$ to 12 times that of a single ${}^1\text{H}$ spin. Because we remove the need to accurately measure frequency offsets, however, simplicity (and potentially accuracy) is enhanced. It is important to choose the correct disentangling sequence so that all MSSM peaks are measured simultaneously, for reasons that will now be discussed.

We can extract many times more information with a single scan by considering all the peaks in the spectrum. A single NOON state sensor can easily encounter aliasing problems; in effect one already needs to know the approximate field offset to be certain of the results. A full arsenal of MSSM states provides a mechanism to avoid such problems. On a quantum sensor with N outer spins, a ϕ phase rotation on the outermost peak could only be aliased with a rotation of $\phi + 2kN\pi$ for some integer k . In quantum interferometric terms [27], such a sensor simultaneously displays both local and global phase distinguishability. Such anti-aliasing effects are a desirable property of these highly symmetric sensor molecules.

For even more sensitive measurement, larger sensors can be employed, potentially with iterative (or other) geometries. To extract information from the outermost peaks of such very large sensors, polarisation amplification methods such as Dynamic Nuclear Polarisation [28] can be applied in addition to the methods outlined above. All sensors can benefit from both the simplified field estimation afforded by disentanglement methods, and from polarisation-priming the pseudo-entanglement resource as introduced in this letter.

In conclusion, we have generated 13-spin pseudo-‘cat’ states for entanglement-enhanced magnetometry. We have proposed and applied innovations to improve the stability and resolution of the entanglement resource. Errors arising from imperfect knowledge of system variables are removed by two different disentanglement methods, and the overall weighted enhancement afforded by polarisation-priming shows approximately a 60-fold increase in the most sensitive components of the sensor.

This research is supported by the EPSRC through the QIP IRC www.qipirc.org (GR/S82176/01) and CAESR (EP/D048559/1). The authors thank Vasileia Filidou for graphics assistance. S.S. thanks Magdalen College, Oxford. J.J.L.M. thanks St. John’s College, Oxford and the Royal Society.

METHODS

The sample was a 1:1 by volume solution of tetramethylsilane and acetone- d_6 , degassed using freeze-pump-thaw cycles, and flame sealed in a 5 mm Wilmad LabGlass NMR tube. All NMR experiments were performed at a temperature of 20°C on a Varian INOVA 600 spectrometer using a broadband tunable X{H} probe with a ^2H lock with a 4-step phase cycle to cancel receiver errors. $\pi/2$ pulse lengths were approximately 27 μs on the hydrogen channel and 17 μs on the silicon channel. The spin-spin coupling $^3J_{\text{SiH}}$ was 6.63 Hz. Measured ^{29}Si relaxation times were $T_2 = 1.2\text{ s}$ and $T_1 = 25.4\text{ s}$, while ^1H relaxation times were $T_2 = 1.6\text{ s}$ and $T_1 = 8.9\text{ s}$.

Quantum logic gates were implemented using standard NMR techniques [14]. Hadamard gates were applied as

$\pi/2_{-y}\pi_z$. C-NOT gates, equivalent to a controlled-phase gate surrounded by Hadamard gates on one channel [14], were implemented as two ^1H $\pi/2$ pulses separated by a spin echo of length $1/2J$, where J is the spin-spin coupling constant. All Z gates were realised as phase shifts in the pulses that followed [14]. To reduce off-resonance and RF inhomogeneity errors, spin-echoes were constructed with two simultaneous π_x pulses at times $1/8J$ and $3/8J$, and all pulses were implemented as simultaneous, equal-duration BB1 composite pulses [29]. Implementing such pulses used suitable amplitude adjustments and ‘0-degree’ identity gate pulses where required.

Data was apodised with a Hamming filter and Fourier transformed using matNMR [30] version 3.9.59. The spectra with no phase accumulation delay was phased, and that phase correction was applied to all other spectra for consistency. Spectra were then exported to Matlab for final processing.

* Electronic address: stephanie.simmons@magd.ox.ac.uk

- [1] B. Yurke, Phys. Rev. Lett. **56**, 1515 (1986).
- [2] V. Giovannetti, S. Lloyd, and L. Maccone, Science **306**, 1330 (2004).
- [3] M. J. Holland and K. Burnett, Phys. Rev. Lett. **71**, 1355 (1993).
- [4] P. Walther, J.-W. Pan, M. Aspelmeyer, R. Ursin, S. Gasparoni, and A. Zeilinger, Nature **429**, 158 (2004).
- [5] M. W. Mitchell, J. S. Lundeen, and A. M. Steinberg, Nature **429**, 161 (2004).
- [6] P. Kok, S. L. Braunstein, and J. P. Dowling, Journal of Optics B: Quant. Semiclass. Opt. **6**, S811 (2004).
- [7] A. N. Boto, P. Kok, D. S. Abrams, S. L. Braunstein, C. P. Williams, and J. P. Dowling, Phys. Rev. Lett. **85**, 2733 (2000).
- [8] M. Riebe, T. Monz, K. Kim, A. S. Villar, P. Schindler, M. Chwalla, M. Hennrich, and R. Blatt, Nature **4**, 839 (2008).
- [9] E. Knill, R. Laflamme, and G. J. Milburn, Nature **409**, 46 (2001).
- [10] M. Hein, J. Eisert, and H. J. Briegel, Phys. Rev. A **69**, 062311 (2004).
- [11] D. G. Cory, A. F. Fahmy, and T. F. Havel, Proc. Natl. Acad. Sci. USA **94**, 1634 (1997).
- [12] N. A. Gershenfeld and I. L. Chuang, Science **275**, 350 (1997).
- [13] E. Knill, I. Chuang, and R. Laflamme, Phys. Rev. A. **57**, 3348 (1998).
- [14] J. A. Jones, Prog. Nucl. Magn. Reson. Spectrosc **38**, 325 (2001).
- [15] J. A. Jones, S. D. Karlen, J. Fitzsimons, A. Ardavan, S. C. Benjamin, G. A. D. Briggs, and J. J. L. Morton, Science **324**, 1166 (2009).
- [16] M. H. Levitt, *Spin Dynamics: Basics of Nuclear Magnetic Resonance*; 2nd ed. (Wiley, Chichester, 2001).
- [17] A. Luis and L. L. Sánchez-Soto, Opt. Comm. **89**, 140 (1992).
- [18] J. J. . Bollinger, W. M. Itano, D. J. Wineland, and D. J.

- Heinzen, Phys. Rev. A **54**, R4649 (1996).
- [19] P. Cappellaro, J. Emerson, N. Boulant, C. Ramanathan, S. Lloyd, and D. G. Cory, Phys. Rev. Lett. **94**, 020502 (2005).
 - [20] E. Knill, R. Laflamme, R. Martinez, and C.-H. T'Seng, Nature **404**, 368 (2000).
 - [21] C. Negrevergne, T. S. Mahesh, C. A. Ryan, M. Ditty, F. Cyr-Racine, W. Power, N. Boulant, T. Havel, D. G. Cory, and R. Laflamme, Phys. Rev. Lett. **96**, 170501 (2006).
 - [22] D. Leibfried, E. Knill, S. Seidelin, J. Britton, R. B. Blakestad, J. Chiaverini, D. B. Hume, W. M. Itano, J. D. Jost, C. Langer, et al., Nature **438**, 639 (2005).
 - [23] M. S. Anwar, D. Blazina, H. A. Carteret, S. B. Duckett, T. K. Halstead, J. A. Jones, C. M. Kozak, and R. J. K. Taylor, Phys. Rev. Lett. **93**, 040501 (2004).
 - [24] J. Baugh, O. Moussa, C. A. Ryan, A. Nayak, and R. Laflamme, Nature **438**, 470 (2005).
 - [25] O. W. Sørensen, Prog. Nucl. Magn. Reson. Spectrosc **21**, 503 (1989).
 - [26] G. A. Morris and R. Freeman, J. Am. Chem. Soc. **101**, 760 (1979).
 - [27] G. A. Durkin and J. P. Dowling, Phys. Rev. Lett. **99**, 070801 (2007).
 - [28] A. W. Overhauser, Phys. Rev. **92**, 411 (1953).
 - [29] H. K. Cummins, G. Llewellyn, and J. A. Jones, Phys. Rev. A. **67**, 042308 (2003).
 - [30] J. D. van Beek, J. Magn. Res. **187**, 19 (2007).